Theoretical Investigation of the Reactivity of Copper Atoms with OCS: Comparison with CS_2 and CO_2

Yana Dobrogorskaya,[†,‡] Joëlle Mascetti,[†] Imre Pápai,[§] and Yacine Hannachi*[,†]

Laboratoire de Physico-Chimie Moléculaire (UMR 5803 CNRS), Université Bordeaux I, 351, cours de la Libération, F-33405 Talence Cedex, France, Chemistry Department, Moscow State University, Moscow, 119899 Russia, and Theoretical Chemistry Department, Institute of Structural Chemistry, Chemical Research Center of HAS, Pusztaszeri út 59-67, H-1025 Budapest, Hungary

Received: May 30, 2005; In Final Form: July 11, 2005

The reaction mechanism of the Cu atom with OCS and CO_2 has been studied by means of density functional method (B3LYP). The overall energetics has been refined at the CCSD(T) level. In the case of the Cu + OCS reaction, the CS insertion route is found much more favorable than the CO insertion one. This later reaction is direct and involves an activation energy of 83.3 kcal/mol and is endothermic by 50.0 kcal/mol at the CCSD(T) level. The insertion into the CS bond proceeds through the η^1_s and η^2_{cs} coordination species as intermediates and is found exothermic by about 20 kcal/mol. The highest transition structure along this route is only 11.5 kcal/mol higher in energy than the reactant's ground states. In the case of the Cu + CO_2 reaction, the insertion route into the CO bond is also found direct but with a lower endothermicity (30.6 kcal/mol) and smaller activation energy (61.1 kcal/mol) than that into the CO bond of OCS. In all cases, the insertion mechanism proceeds simultaneously with electron transfer from the Cu atom to OCS (or CO_2) molecule.

(1) Introduction

Because the organometallic chemistry of heteroallene molecules plays an important role in catalysis, biochemistry, and material science,[1] work in our research group is focused on the reactivity of transition metal atoms with CO_2, OCS, and CS_2, both experimentally, by matrix isolation spectroscopy, and theoretically, through DFT and ab initio methods. Our recent density functional study on the V + CO_2, CS_2, and OCS reactions[2] has compared the insertion process for the three molecules and has pointed out the differences in the energetics which have been related to the molecular properties of the reactants. In all cases, the insertion products have been calculated to be more stable than the corresponding coordination complexes. The η^2_{cs}-V(OCS) complex has not been identified as a minimum on the V + OCS potential energy surface as we found no energy barrier for the metal insertion into the C−S bond. Usually, early transition metal atoms are known to undergo an easy insertion process, whereas late ones are supposed to form coordination complexes more readily.

To our knowledge, no matrix isolation study has been devoted to the reactions of copper and OCS. Recently, guided ion beam gas studies by Armentrout et al.[3] on Cu^+ + OCS have indicated that both the ground state (^1S) and first excited state (^3D) of Cu^+ are formed and the ground-state ions undergo endothermic reactions to form CuS^+ and $CuCO^+$. The authors suggested that the initial mechanistic step corresponds to the insertion of Cu^+ into the CS bond of OCS.

In our previous matrix study on the reactions of CO_2 with thermally evaporated copper atoms,[4] only one coordination complex, the end-on η^1_o-Cu(CO_2) species was observed in pure CO_2, whereas no reaction occurred in argon dilute deposits. Subsequent ab initio calculations by Caballol et al.[5] showed that the η^2_{co}-Cu(CO_2) side-on complex was a weak van der Waals species, whereas the end-on complex (η^1_O−Cu(CO_2)) was characterized by an important charge transfer from copper to the CO_2 moiety but being very close in energy to η^2_{co}-Cu(CO_2). More recently, Andrews et al. published a combined matrix isolation−DFT study on the reactions of laser ablated Cu atoms and CO_2.[6] Due to the higher kinetic and possibly electronic energy of copper atoms, the reactivity was more important and two anionic species were observed: the C-coordinated complex $CuCO_2^-$ and the insertion product $OCuCO^-$. It is worth noting that no neutral species has been identified under these experimental conditions.

In the present work, we complete our previous studies on Cu + CS_2 [7] and Cu + CO_2 [4] in order to compare the reactivity of early and late transition metals toward these three molecules. The paper is organized as follows. Computational details are listed in section 2. We present in section 3 the assessment of the computational methods used in this work, then we describe the minima found along the Cu + OCS and Cu + CO_2 surfaces and the mechanisms for three reactions: Cu + OCS → CuS + CO, Cu + OCS → CuO + CS, and Cu + CO_2 → CuO + CO. The comparison of reactivity of copper atoms toward heteroallenes (CO_2, CS_2, OCS) is made in the last part of section 3, together with a comparison with available experimental data and previous results obtained on the reactivity of an early transition metal, vanadium.[2]

(2) Computational Details

All calculations in the present study were performed using the Gaussian98 program.[8] The stationary points on the potential energy surfaces were located using B3LYP density functional

* To whom correspodence should be addressed. Fax: (33) 5-40-00-66-45. E-mail: y.hannachi@lpcm.u-bordeaux1.fr.
† Université Bordeaux I.
‡ Moscow State University.
§ Chemical Research Center of HAS.

10.1021/jp052853p CCC: $30.25 © 2005 American Chemical Society
Published on Web 08/12/2005

calculations.[9−11] Two basis sets have been chosen for these calculations. The first one includes the (14,9,5)/[8,5,3] all-electron Cu basis set of Schäfer, Horn, and Ahlrichs[12] supplemented with two polarization p functions[13] and a diffuse d function[14] and the 6-311+G(2d) basis set for carbon, sulfur, and oxygen.[15] This basis set will be referred to as 6-311+G-(2d) in this paper for simplicity. The second one is derived from the standard 6-311+G(3df) set[16] by omitting the g polarization functions from the Cu basis. This set will hereafter be denoted as 6-311+G(3df)′. Calculations with the standard 6-311+G-(3df) basis set led to an unphysical symmetry breaking of the molecular orbitals, which was not observed when the g functions were omitted from the basis set. Only the structural parameters and relative energies obtained at the B3LYP/6-311+G(3df)′ level will be presented and discussed; the ones obtained at the B3LYP/6-311+G(2d) level are very similar.

For each stationary point, we carried out single-point CCSD-(T)/6-311+G(3df)′//B3LYP/6-311+G(3df)′ energy calculations.[17,18] The correlation treatment in the coupled cluster calculations involved all valence electrons. The restricted and the unrestricted formalism are applied for closed shell and open shell, respectively. The lowest energy solution for each stationary point is obtained and checked through a stability test. The vibrational frequencies were calculated at the B3LYP/6-311+G-(2d) and B3LYP/6-311+G(3df)′ levels for each stationary point and served as data to estimate the zero-point energies (ZPE) (without scaling) and also to characterize the nature of the stationary points (minimum vs first-order saddle point). In the CCSD(T) calculations, we applied the unscaled B3LYP/6-311+G(3df)′ ZPE corrections. To verify whether the located transition states connect the expected minima, intrinsic reaction coordinate (IRC) calculations[19] were carried out in both directions from each transition state at the B3LYP/6-311+G(2d) level with a step size of 0.1 amu$^{1/2}$ bohr. The atomic populations (atomic charges, electron configuration, etc.) were derived from natural bond orbital (NBO) analysis[20] carried out for the relevant structures at the B3LYP/6-311+G(3df)′ level.

(3) Results and Discussion

The optimized stationary points are shown in Figures 1 and 2. Figures 3, 4, and 5 report the schematic reaction mechanisms with the relative energies of the reactants, products, intermediate species, and transition structures obtained at the B3LYP and CCSD(T) levels. The corresponding B3LYP harmonic vibrational frequencies and infrared intensities are listed in Table 1.

3.1. Assessment of the Computational Methods. On the basis of the experimental Cu−S bond strength in CuS diatomic (64.6 kcal/mol) [21] and the experimental heats of formation of copper (80.4 kcal/mol) and sulfur atoms (65.6 kcal/mol) at 0 K,[22] ΔH_f for CuS is 81.4 kcal/mol. With this value and experimental ΔH_f for Cu, OCS (−33.1 kcal/mol) and CO (−27.2 kcal/mol),[22] the Cu + OCS → CuS + CO reaction is found to be endothermic by 6.9 kcal/mol. The calculated value depends on how the thermochemistry for the Cu + S → CuS and OCS → CO + S reactions is reproduced. For the Cu−S bond strength of CuS, the B3LYP and CCSD(T) values are 61.8 and 59.2 kcal/mol, respectively, which are close to the theoretical values obtained by Bauschlicher and Maître (in the range of 57.4−61.6 kcal/mol)[23] but underestimate the experimental value by 2.8 and 5.4 kcal/mol, respectively. The calculated reaction energies for OCS → CO + S are 75.5 (B3LYP) and 68.5 (CCSD(T)) kcal/mol and compare well with the experimental value of 71.5 kcal/mol. The combination of the thermochemistry of the two above reactions gives the reaction energy for Cu + OCS → CS + CuS. The B3LYP method gives 13.7 kcal/mol while CCSD(T) is in a better agreement with a value of 9.3 kcal/mol (see Figure 3). In the same manner, the experimental Cu + OCS → CuO + CS reaction energy is 94.0 kcal/mol.[21,22] The B3LYP method gives 101.1 kcal/mol while CCSD(T) is also in a better agreement with a value of 98.2 kcal/mol (see Figure 4). The experimental value for the Cu + CO_2 → CuO + CO is 61.5 kcal/mol, which is close to the computed values (66.5 and 64.5 kcal/mol at the B3LYP and CCSD(T) levels, respectively; see Figure 4). The predicted energies can be considered satisfactory taking into account that the experimental CuS and CuO bond strength are not very accurately known.

The calculated CS bond lengths at the B3LYP level are, respectively, 1.532 Å for CS and 1.563 Å for OCS (see Figure 1) which are very close to the experimental values (1.534 and 1.561 Å respectively).[21,24] In the case of the CO bond lengths, the calculated values are 1.125 (CO), 1.155 (OCS), and 1.159

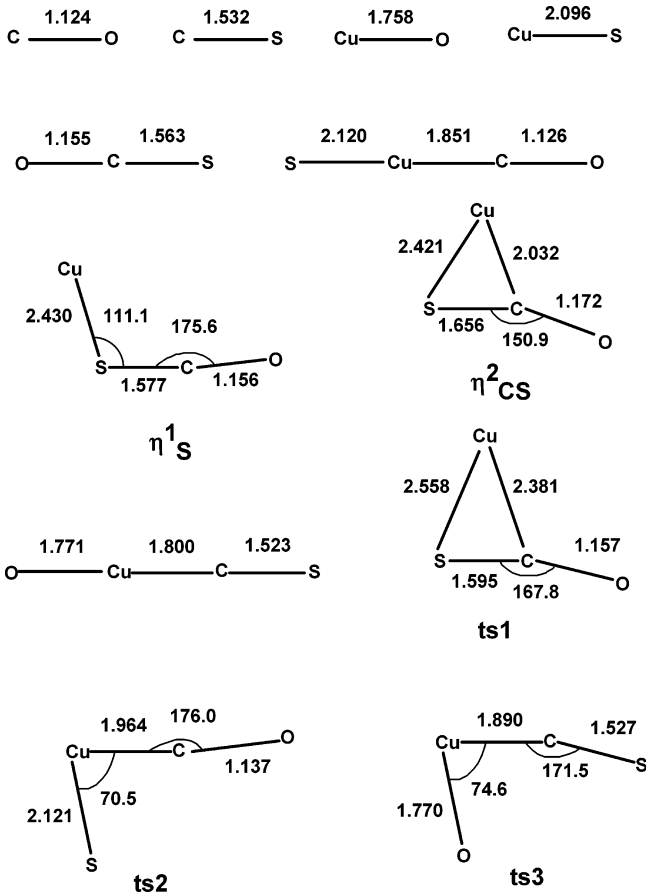

Figure 1. Optimized geometries of the various stationary points located on the Cu + OCS potential energy surface (distances in angstroms, angles in degrees).

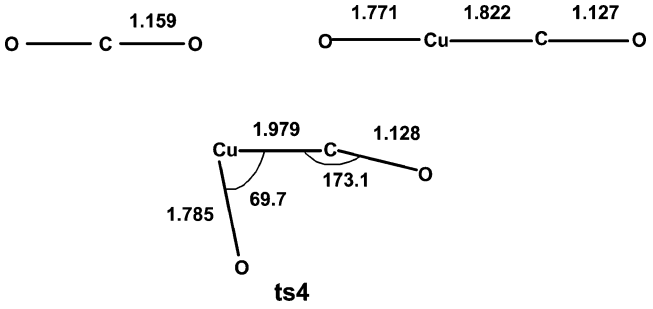

Figure 2. Optimized geometries of the various stationary points located on the Cu + CO_2 potential energy surface (distances in angstroms, angles in degrees).

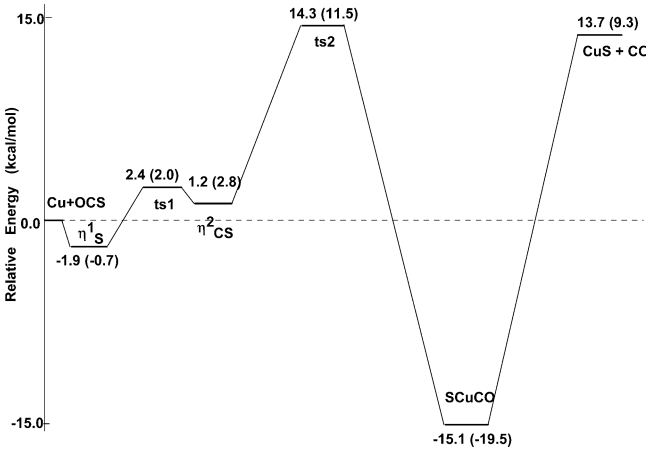

Figure 3. Schematic reaction path of Cu + OCS → CuS + CO with B3LYP/6-311+G(3df)′ and CCSD(T)/6-311+G(3df)′ (single point in parentheses) relative energies.

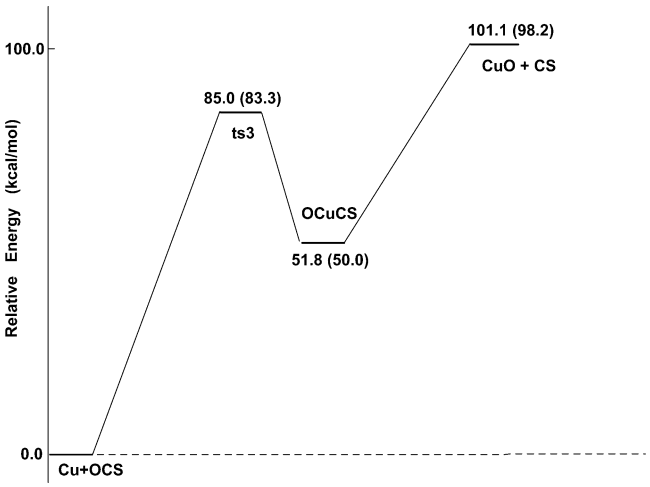

Figure 4. Schematic reaction path of Cu + OCS → CuO + CS with B3LYP/6-311+G(3df)′ and CCSD(T)/6-311+G(3df)′ (single point in parentheses) relative energies.

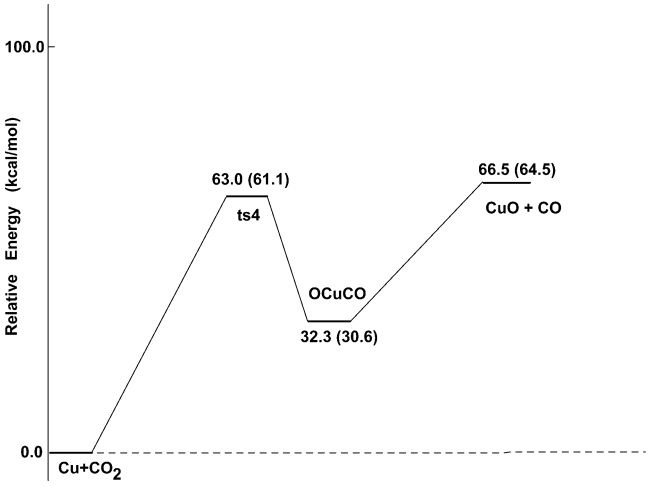

Figure 5. Schematic reaction path of Cu + CO_2 → CuO + CO with B3LYP/6-311+G(3df)′ and CCSD(T)/6-311+G(3df)′ (single point in parentheses) relative energies.

Å (CO_2) which are in line with the corresponding experimental values (1.128, 1.156, and 1.162 Å, respectively).[21,25] A nice agreement also holds for the calculated vibrational frequencies. The calculated (experimental) values are 1312 (1285 cm^{-1}) for CS, 2217 (2170 cm^{-1}) for CO, 2116, 880, and 531 (2072, 866, and 520 cm^{-1}) for OCS, and 2414, 1374, and 679 (2349, 1333, and 667 cm^{-1}) for CO_2.[21,24,26] The situation is a bit less favorable for the CuS and CuO molecules. The calculated bond lengths are, respectively, 2.103 and 1.758 Å, and the harmonic vibrational frequencies are 388 and 611 cm^{-1}, which should be compared to the experimental values of 2.051 and 1.725 Å and 415 and 640 cm^{-1}, respectively.[21]

TABLE 1: Calculated Vibrational Frequencies (cm^{-1}) and IR Intensities (km/mol) of the Different Stationary Points on the Cu + OCS and Cu + CO_2 Potential Energy Surfaces[a]

species	frequency (IR intensity)
η^1_s (C_s, $^2A'$)	68 (1), 138 (2), 437 (96), 502 (7), 833 (10), 2078 (1347)
η^2_{cs} (C_s, $^2A'$)	137 (14), 229 (1), 402 (511), 434 (1), 684 (151), 1902 (660)
SCuCO ($C_{\infty v}$, $^2\Pi$)	65 (5), 70 (4), 339 (1), 340 (22), 369 (4), 441 (1), 2203 (735)
OCuCS($C_{\infty v}$, $^2\Pi$)	75 (8), 79 (5), 303 (11), 346 (6), 366 (11), 637 (20), 1418 (455)
OCuCO($C_{\infty v}$, $^2\Pi$)	89 (16), 96 (13), 365 (0), 402 (1), 413 (22), 643 (10), 2209 (560)
CuO($C_{\infty v}$, $^2\Pi$)	611 (10)
CuS($C_{\infty v}$, $^2\Pi$)	388 (3)
CO($C_{\infty v}$, $^1\Sigma^+$)	2217 (80)
CS($C_{\infty v}$, $^1\Sigma^+$)	1312 (87)
OCS($C_{\infty v}$, $^1\Sigma^+$)	531 (2), 531 (2), 880 (10), 2116 (770)
CO_2($D_{\infty h}$, $^1\Sigma_g^+$)	679 (32), 679 (32), 1374 (0), 2414 (677)
ts1 (C_s, $^2A'$)	167*i* (153), 103 (7), 289 (238), 486 (0), 795 (38), 2157 (526)
ts2 (C_s, $^2A'$)	272*i* (81), 210 (1), 222 (3), 309 (1), 385 (15), 2079 (611)
ts3 (C_s, $^2A'$)	419*i* (103), 163 (8), 179 (18), 309 (3), 572 (9), 1359 (375)
ts4 (C_s, $^2A'$)	324*i* (80), 180 (0), 226 (1), 270 (6), 565 (10), 2167 (394)

[a]The vibrational frequencies are unscaled.

3.2. Minima. Among the different possible coordination modes,[1,27,28] two minima, namely, the η^1_s (C_S, $^2A'$) and the η^2_{cs} (C_S, $^2A'$) species have been located on the Cu + OCS potential energy surface (PES) (see Figure 1). Our attempts to locate the η^1_o, η^1_c, η^2_{os}, and η^2_{co} species converged either to the located coordination compounds or to the separate reactants. In addition, both the CO and CS insertion products ($C_{\infty}v$, $^2\Pi$) have been located on the PES.

In contrast to the Cu + CS_2 system,[7] the most stable species is the CS insertion product SCuCO which is found about 20 kcal/mol lower in energy than the reactants ground states at the CCSD(T) level. The η^1_s species is very weakly bound (1.9 and 0.7 kcal/mol at the B3LYP and CCSD(T) level, respectively). The η^2_{cs} species is found higher in energy than the separate reactants by 1.8 and 2.8 kcal/mol at the B3LYP and CCSD(T) levels, respectively. The highest energy isomer is the CO insertion product, OCuCS ($C_{\infty}v$, $^2\Pi$), about 50 kcal/mol higher in energy than the reactants.

On the Cu + CO_2 PES, only the CO insertion product, OCuCO ($C_{\infty}v$, $^2\Pi$), could be located at the B3LYP level. Another minimum, the η^1_c ($^2A_2$) species, has also been obtained. It is calculated 70.3 kcal/mol higher in energy than the reactants ground states at the CCSD(T) level. However, a stability test revealed a lower solution, $^2A_1$, at the same geometry, some 25 kcal/mol lower in energy at the B3LYP/6-311+G(2d) level. The optimization with this new solution leads to separate reactants. Our findings contrast with the previous study of Caballol et al.,[5] where the η^2_{co} ($^2A'$), η^1_o ($^2A'$), η^2_{oo} ($^2A_1$), and η^1_c ($^2A_2$) species have been located at a moderate level of CI theory and the obtained stabilities relative to the reactants ground states were −5.9, −4.5, 8.3, and 46.1 kcal/mol, respectively. Except

for the η^1_c species as mentioned previously, all our attempts to locate these species lead to separate reactants. Several other functionals have been tested and found to yield the same scheme as B3LYP. It seems that the DFT methodology is unable to account for the bonding in these weakly bound complexes. A proper description of van der Waals complexes involving transition metals needs a multiconfiguration based approach including dynamical correlation, that is, MRCI or CASPT2 with a large basis set. Work along this line is in progress in our group. Nevertheless, our results on the Cu + CO_2 system are interesting for the sake of comparison of the insertion reaction among the CXY (X = O, S) systems.

3.3. Description of Reactions Mechanisms. (a) Cu + OCS → CuS + CO. The entrance channel of this reaction is barrierless and proceeds through the formation of a η^1_s species as a reaction intermediate (see Figures 1 and 3). As mentioned in the previous section, this species is only weakly bound with respect to the reactants. The OCS moiety is slightly perturbed with a 0.014 Å increase of the CS bond and 4.4° decrease of the OCS angle, while the CO bond is virtually unchanged. The CuS bond length in this complex is 2.430 Å, about 0.3 Å larger than that in the CuS diatomic, which is essentially a single bond.[23] The NBO analysis shows that, in comparison with separate reactants, the atomic charge on the Cu atom increases up to only 0.07 e, whereas the atomic charge on the S atom decreases down to −0.05 e (it is 0.03 in isolated OCS). The electronic configuration of the Cu atom in the η^1_s complex is 4s(0.98)3d(9.95), which means that the electronic configuration of this complex correlates directly to that of the ground-state reactants. This situation is very similar to that of the same complex in the Cu + CS_2 system, [7] but this complex is less stable with respect to the ground-state reactants in the present case. The next step corresponds to the $\eta^1_s \rightarrow \eta^2_{cs}$ isomerization. This involves an activation barrier of 4.3 and 2.7 kcal/mol at the B3LYP and CCSD(T) levels, respectively, and it is endothermic. The corresponding transition structure is denoted ts1 in Figures 1 and 3. While the η^2_{cs} species is 1.2 kcal/mol lower in energy than ts1 at the B3LYP level, single-point calculation at the CCSD(T) level puts ts1 0.8 kcal/mol lower. This shows that the PES is flat in the corresponding region. In addition, inspection of the T1 diagnostic[29] of the CCSD wave function shows that ts1 is, surprisingly, better described by a single reference wave function than the η^2_{cs} species (lower T1 value). We expect that a full optimization at the CCSD(T) level will put ts1 higher in energy than the η^2_{cs} complex. However, the PES in this region is flat, which means that the reverse isomerization will be very fast in the gas phase. The NBO analysis shows that when going from η^1_s to ts1, the atomic charges are very slightly modified (decrease of the S and C atomic charges and increase of the Cu one). The OCS subunit starts to bend to reach an angle of about 168°, and the CS bond length increases by about 0.02 Å. A more significant change is observed when going from ts1 to the η^2_{cs} complex. The atomic charge of Cu increases from 0.07 e to 0.38 e, whereas the atomic charge on S decreases from −0.05 e to −0.12 e and that on the C atom decreases from 0.41 e to 0.20 e. We also observe significant changes in the geometrical parameters of OCS. The CS and CO bond lengths increase by 0.1 and 0.02 Å, respectively, whereas the OCS angle decreases to about 151°. The next step in the reaction mechanism is the insertion of the Cu atom into the CS bond producing a linear SCuCO molecule ($^2\Pi$). This step is exothermic by about 22 kcal/mol and requires an activation energy of about 9 kcal/mol at the CCSD(T) level. The insertion species, SCuCO, is calculated as 19.5 kcal/mol more stable than the reactants. The corresponding transition structure, called ts2, is only 11.5 kcal/mol higher in energy than the reactants. This is the rate-limiting step along the insertion route as it involves the highest lying transition structure. The NBO analysis shows that, when going from the η^2_{cs} to ts2, there is a large charge transfer from the sulfur atom to the Cu atom as the corresponding atom charges become in ts2, respectively, −0.65 e and 0.80 e. This mainly comes from the unpaired electron on the Cu atom as the Cu electronic configuration changes from 4s(0.75)3d(9.84) in η^2_{cs} to 4s(0.38)3d(9.78) in ts2. Back-donation is observed when going from ts2 to the insertion species with a decrease of the atomic charge on Cu and an increase of the atomic charges on the S and C atoms. This situation is similar to the case of the insertion of nickel and scandium atoms into CO_2[30,31] where the insertion mechanism features, the oxygen abstraction and metal insertion, take place simultaneously with electron transfer. This mechanism has also been proposed for the reactions of NO_2 and N_2O molecules with 3d transition metals.[32] The insertion species, SCuCO, may dissociate without an exit barrier to CO and CuS ground states as shown in Figure 3. This step is endothermic by 28.8 kcal/mol which puts CO + CuS 9.3 kcal/mol higher than Cu + OCS at the CCSD(T) level.

(b) Cu + OCS → CuO + CS. As mentioned previously, we could not locate any η^1_o or η^2_{co} coordination species on the Cu + OCS PES. For this reason, the insertion mechanism is direct and involves only one step. The insertion transition structure, named ts3, is located 83.3 kcal/mol above the reactants at the CCSD(T) level. The IRC calculations carried out from ts3 confirmed that this transition state connects OCuCS to Cu + OCS directly. The CO insertion reaction is found to be endothermic, with OCuCS being 50.0 kcal/mol higher than Cu + OCS. As in the case of CS insertion route, the NBO analysis shows that a large charge transfer from the Cu atom to OCS occurs from the reactants to ts3. In ts3, the Cu atom charge is 1.02 e, that of the O atom is −0.9 e, that of the C atom is −0.44 e, and that of the S atom is 0.32 e. (The values for the O, C, and S atoms in isolated OCS are respectively −0.44, 0.41, and 0.03 e.) A back-donation occurs from ts3 to OCuCS. In the insertion species, the Cu atomic charge drops back to 0.83 and that of the O atom drops to −0.73. This is very similar to the insertion mechanism discussed in the previous section. As in the case of SCuCO, OCuCS may dissociate without a barrier to CuO + CS. This reaction is endothermic by 48.2 kcal/mol at the CCSD(T) level which puts CuO + CS almost 100 kcal/mol above Cu + OCS.

(c) Cu + CO_2 → CuO + CO. The insertion mechanism in the present case is very similar to that of Cu insertion into the CO bond of OCS. This process is direct and involves a single step but requires less energy than that for OCS. The corresponding transition structure, named ts4, is located 61.1 kcal/mol above Cu + CO_2 at the CCSD(T) level. The insertion reaction is endothermic by 30.6 kcal/mol. The NBO analysis shows the same features as in the case of Cu insertion into CO or CS bond of OCS. A large charge transfer from the Cu atom to CO_2 occurs from the reactants to ts4. In ts4, the Cu atom charge is 0.94 e, that of the O atom bonded to Cu is −0.92 e, that of the C atom is 0.43 e, and that of the terminal O atom is −0.43 e. (The values for O and C in isolated CO_2 are, respectively, −0.5 and 1.0 e.) A back-donation occurs from ts4 to OCuCO. In the insertion species, the Cu atomic charge drops back to 0.74 and that of the O atom bonded to Cu drops to −0.74 e, while the atomic charges of the C and terminal O atoms do not change significantly (0.41 and −0.43 e, respectively).

The difference in electronegativity between the S atom and the O atom makes the C atom positively charged and the O atom negatively charged ts4 and OCuCO, respectively, while the C atom is negatively charged and the S atom positively charged in ts3 and OCuCS. The OCuCO species may also dissociate to CuO + CO without a barrier. This reaction is endothermic by about 34 kcal/mol at the CCSD(T) level.

(d) Other Possible Exit Channels. Experimental studies on gas-phase reactions of Cu^+ with OCS reveal the importance of the $(CuS)^+$ + CO and the S + $(CuCO)^+$ exit channels.[3] Although we are concerned with neutral species in this work, we also investigate possible exit channels besides the CuO + CS and CuS + CO in the case of the Cu + OCS reaction and CuO + CO in the case of the Cu + CO_2 reaction. In principle, the insertion products SCuCO and OCuCS could lead to S + CuCO or O + CuCS by the cleavage of one of the terminal bonds. Our calculations indicate that the Cu + OCS → S (^{3}P) + CuCO (^{2}A′) is endothermic by 65.4 kcal/mol at the CCSD(T) level. In addition, the SCuCO species can dissociate without barrier to S (^{3}P) + CuCO (^{2}A′). This puts this exit channel as the next most favorable besides CuS + CO in the case of the Cu + OCS reaction. The OCuCS species can also dissociate without barrier to O (^{3}P) + CuCS (^{2}A′), but the Cu + OCS → O + CuCS reaction is much more endothermic (136.9 kcal/mol at the CCSD(T) level). The CCuO and CCuS species are less stable than CuCO and CuCS, respectively, so the corresponding exit channels are much higher in energy. Finally, the Cu + OCS → CuC ($^4\Sigma^-$) + SO ($^3\Sigma^-$) reaction is found endothermic by 156.3 kcal/mol at the CCSD(T) level whereas the Cu + OCS → C (^{3}P) + CuOS (^{2}A″) reaction is about 17 kcal/mol higher (176.2 kcal/mol).

In the case of the Cu + CO_2 reaction, we found that the OCuCO insertion species can dissociate without exit barrier to O(^{3}P) + CuCO (^{2}A′). The Cu + CO_2 → O(^{3}P) + CuCO (^{2}A′) reaction is endothermic by 119.6 kcal/mol at the CCSD(T) level, about 55 kcal/mol more than the most favorable channel (CO + CuO). The Cu + CO_2 → CuC ($^4\Sigma^-$) + O_2 ($^3\Sigma^-_g$) reaction is found endothermic by 214.7 kcal/mol at the CCSD(T) level whereas the Cu + CO_2 → C (^{3}P) + CuO_2 ($^2A_2$) reaction is about 35 kcal/mol higher (249.3 kcal/mol).[33,34]

These results show that the most favorable exit channel in the case of the Cu + OCS reaction is the one leading to CuS + CO followed by the one leading to S + CuCO. For the Cu + CO_2 reaction, the most favorable exit channel is the one leading to CuO + CO followed by the one leading to O + CuCO.

3.4. Comparison of Reactions of Cu and V with CO_2, CS_2, and OCS. For the Cu + XCY systems (X, Y = O, S), the most favorable reaction channel proceeds through an insertion elimination process producing CuX + CY. The insertion into the CO bond of CO_2 is more favorable than the insertion into the CO bond of OCS. The insertion species and the transition state are more stable in the case of CO_2 by about 20 kcal/mol with respect to the reactant's ground states. The situation is reversed in the case of the insertion into the CS bond, which is more favorable in the case of OCS as compared to CS_2.[7] This is consistent with the relative CO bond strengths in CO_2 and OCS and the relative CS bond strengths in CS_2 and OCS.[22] The relative stabilities of the insertion products XCuCY (X, Y = O, S) relative to the Cu + XCY asymptotes vary in the [−20, +50] kcal/mol energy range, and the order of decreasing stability is SCuCO (−19.5), SCuCS (−1.3), OCuCO (30.6), and OCuCS (50 kcal/mol). SCuCS and SCuCO are about 50 kcal/mol more stable than OCuCS and OCuCO, respectively. The insertion species XCuCY might be characterized as XCu−CY complexes. It is thus interesting to determine their XCu−CY binding energy. The obtained values (the energy of the XCuCY → CuX + CY reactions) are 28.8 (SCuCO), 33.9 (OCuCO), 43 (SCuCS), and 48.2 kcal/mol (OCuCS). As a general trend, one observes that the XCu−CO bonds are about 14 kcal/mol less stable than the corresponding XCu−CS bonds, whereas the CO and CS molecules form about 5 kcal/mol stronger bonds with CuO than with CuS.

In a previous work, the insertion mechanism of the vanadium atom into CO_2, OCS, and CS_2 has been presented.[2] The comparison of the reactivity of vanadium with the three heteroallenes shows similar trends as observed with a copper atom. However, the insertion species in the case of vanadium are much more stable with respect to the reactants. The insertion products into the CO and CS bonds are, respectively, about 70 and 35 kcal/mol more stable in the case of the vanadium species. The situation is similar when the stability of the insertion transition states are considered. The MO + CY and MS + CY asymptotes are about 83 and 38 kcal/mol lower in energy with respect to M + XCY in the case of vanadium when compared to the copper case. The V + XCY → VX + CY reaction is thus much more favorable than the Cu + XCY → CuX + CY reaction. This is directly related to the bond strengths of the MO and MS diatomics, which decrease from early to late first row transition metals.[21,23] Another difference between the vanadium system and that of the copper one is that CO and CS molecules form about 6−7 kcal/mol stronger bonds with VS than with VO, whereas the situation is reversed in the case of copper as already mentioned above. This might, however, not be a general trend between early and late first row transition metals oxides (sulfides).

(4) Concluding Remarks

The title reactions have been studied at the B3LYP and CCSD(T) levels. The insertion reaction of Cu atoms in the CS bond of OCS is found much more favorable than the insertion into its CO bond. The CS insertion reaction is about 20 kcal/mol exothermic and proceeds through the formation of an end-on (η^1_S) and a side-on (η^2_{CS}) coordination compound. The highest transition structure along the insertion route is found about 11 kcal/mol higher in energy than Cu + OCS. The overall Cu + OCS → CuO + CS reaction is calculated as about 9 kcal/mol endothermic, close to the experimental value (7 kcal/mol). The Cu + OCS insertion reaction has been compared with Cu + CO_2 and Cu + CS_2, and similar trends are observed as for the previously studied V + XCY reactions. However, the Cu reactions are found much less favorable than the vanadium reactions, and this is related to the relative strengths of the metal−oxide or the metal−sulfide bonds.

Similar calculations on the reactivity of the nickel atom with XCY molecules are in progress in order to complete our previous work on Ni + CO_2.[30]

Acknowledgment. This work has been partly supported by an INTAS program (project 00-00911). Y.H. gratefully acknowledges computational facilities provided by the intensive calculation pole "M3PEC-MESOCENTRE" of the University Bordeaux I-DRIMM, partly financed by the Regional Council of Aquitaine. Y.D. gratefully acknowledges financial support from NATO to allow her a 7 month visit to Bordeaux. Financial support from the Hungarian Research foundation (OTKA grant T034547) is also acknowledged.

References and Notes

(1) Pandey, K. K. *Coord. Chem. Rev.* **1995**, *140*, 37.

(2) Pápai, I.; Hannachi, Y.; Gwizdala, S.; Mascetti, J. *J. Phys. Chem. A* **2002**, *106*, 4181.
(3) Rue, C.; Armentrout, P. B.; Kretzschmar, I.; Schröder, D.; Schwarz, H. *J. Phys. Chem. A* **2002**, *106*, 9788.
(4) Mascetti, J.; Tranquille, M. *J. Phys. Chem.* **1988**, *92*, 2177.
(5) Caballol, R.; Sanchez Marcos, E.; Barthelat, J. C. *J. Phys. Chem.* **1987**, *91*, 1328.
(6) Zhou, M.; Liang, B.; Andrews, L. *J. Phys. Chem. A* **1999**, *103*, 2013.
(7) Dobrogorskaya, Y.; Mascetti, J.; Pápai, I.; Nemukhin, A.; Hannachi, Y. *J. Phys. Chem. A* **2003**, *107*, 2711.
(8) Frisch, M. J.; Trucks, G. W.; Schlegel, H. B.; Scuseria, G. E.; Robb, M. A.; Cheeseman, J. R.; Zakrzewski, V. G.; Montgomery, J. A., Jr.; Stratmann, R. E.; Burant, J. C.; Dapprich, S.; Millam, J. M.; Daniels, A. D.; Kudin, K. N.; Strain, M. C.; Farkas, O.; Tomasi, J.; Barone, V.; Cossi, M.; Cammi, R.; Mennucci, B.; Pomelli, C.; Adamo, C.; Clifford, S.; Ochterski, J.; Petersson, G. A.; Ayala, P. Y.; Cui, Q.; Morokuma, K.; Malick, D. K.; Rabuck, A. D.; Raghavachari, K.; Foresman, J. B.; Cioslowski, J.; Ortiz, J. V.; Baboul, A. G.; Stefanov, B. B.; Liu, G.; Liashenko, A.; Piskorz, P.; Komaromi, I.; Gomperts, R.; Martin, R. L.; Fox, D. J.; Keith, T.; Al-Laham, M. A.; Peng, C. Y.; Nanayakkara, A.; Challacombe, M.; Gill, P. M. W.; Johnson, B.; Chen, W.; Wong, M. W.; Andres, J. L.; Gonzalez, C.; Head-Gordon, M.; Replogle, E. S.; Pople, J. A. *Gaussian 98*, revision A.7; Gaussian, Inc.: Pittsburgh, PA, 1998.
(9) Becke, A. D. *J. Chem. Phys.* **1993**, *98*, 5648.
(10) Lee, C.; Yang, W.; Parr, R. G. *Phys. Rev. B* **1988**, *37*, 785.
(11) Stephens, P. J.; Devlin, F. J.; Chabalowski, C. F.; Frisch, M. J. *J. Phys. Chem.* **1994**, *98*, 11623.
(12) Schäfer, A.; Horn, H.; Ahlrichs, R. *J. Chem. Phys.* **1992**, *97*, 2571.
(13) Wachters, A. J. H. *J. Chem. Phys.* **1970**, *66*, 43.
(14) Hay, P. J. *J. Phys. Chem.* **1977**, *66*, 43.
(15) Krishnan, R.; Binkley, J. S.; Seeger, R.; Pople, J. A. *J. Chem. Phys.* **1980**, *72*, 650. Frisch, M. J.; Pople, J. A.; Binkley, J. S. *J. Chem. Phys.* **1984**, *80*, 3265.
(16) See ref 8.
(17) Purvis, G. D.; Bartlett, R. J. *J. Chem. Phys.* **1982**, *76*, 1910.
(18) Pople, J. A., Head-Gordon, M.; Raghavachari, K. *J. Chem. Phys.* **1987**, *87*, 5968.
(19) Gonzalez, C.; Schlegel, H. B. *J. Chem. Phys.* **1989**, *90*, 2154.
(20) Reed, A. E.; Curtiss, L. A.; Weinhold, F. *Chem. Rev.* **1988**, *88*, 899.
(21) Huber, K. P.; Herzberg, G. *Constants of Diatomic Molecules*; Van Nostrand Reinhold: New York, 1979.
(22) Chase, M. W., Jr.; Davies, C. A.; Downey, J. R., Jr.; Frurip, D. J.; McDonald, R. A.; Syverud, A. N. JANAF Tables, 3rd ed.; *J. Phys. Chem. Ref. Data*; 1985; Vol. 14, Suppl. 1.
(23) Bauschlicher, C. W.; Maître, P. *Theor. Chim. Acta* **1995**, *90*, 189.
(24) Lahaye, J. G.; Vanderhaute, R.; Fayt, A. *J. Mol. Spectrosc.* **1987**, *123*, 48.
(25) Herzberg, G. *Molecular Spectra and Molecular Structure III. Electronic Spectra and Electronic Structure of Polyatomic Molecules*; Van Nostrand Reinhold: New York, 1966.
(26) *CRC Handbook of Chemistry and Physics*; Lide, D. R., Ed.; CRC Press: Boca Raton, FL, 1994.
(27) Gibson, D. H. *Chem. Rev.* **1996**, *96*, 2063.
(28) Mascetti, J.; Gallan, F.; Pápai, I. *Coord. Chem. Rev.* **1999**, *190*−*192*, 557.
(29) Lee, T. J.; Taylor, P. R. *Int. J. Quantum Chem. Symp.* **1989**, *23*, 199.
(30) Hannachi, Y.; Mascetti, J.; Stirling, A.; Pápai, I. *J. Phys. Chem. A* **2003**, *107*, 6708.
(31) Pápai, I.; Schubert, G.; Hannachi, Y.; Mascetti, J. *J. Phys. Chem. A* **2002**, *106*, 9551.
(32) Stirling, A. *J. Am. Chem. Soc.* **2002**, *124*, 4058.
(33) The most stable structure of CuO_2 is found the ^{2}A" state at the B3LYP level while the $^2A_2$ state is found a first order saddle point. However, single point calculation at the CCSD(T) level puts the $^2A_2$ state lower in energy, and the entire ^{2}A" ground-state surface is very flat. This is consistent with the CCSD(T) results of Bauschlicher et al.; see ref 34.
(34) Bauschlicher, C. W.; Langhoff S. R.; Partridge, H.; Sodupe, M. *J. Phys. Chem.* **1993**, *97*, 856.